Metamorphosis of caffeine hydrate and anhydrous caffeine

Howell G. M. Edwards,[b] Emma Lawson,[b] Marcel de Matas,[a] Len Shields[b] and Peter York[a]

[a] *Postgraduate studies in Pharmaceutical Technology, School of Pharmacy and*
[b] *Department of Chemistry, University of Bradford, Bradford, UK BD7 1DP*

The phase stability, interconversion and physicochemical characterisation of caffeine (1,3,7-trimethylpurine-2,6-dione) hydrate and anhydrous caffeine relate to the strength of the available hydrogen-bonds. A hydrogen-bonded T-branched spine of hydrate molecules establishes a weak lattice bond for the caffeine hydrate which, under ambient conditions, transforms to a β-anhydrous phase which in turn, at 155 °C and with an enthalpy of 3.6 kJ mol^{-1}, converts to a trigonal phase α-anhydrous caffeine. The anhydrous phases are stabilised by weak CH_3 to CO hydrogen bonds.

Introduction

The phase changes associated with caffeine, 1,3,7-trimethylpurine-2,6-dione, are generally related to the state of hydration of the molecule; one disordered and incommensurate hydrate phase will transform in ambient atmospheric conditions to an anhydrous β-phase which converts at high temperature to a second metastable anhydrous α-phase which subsequently sublimes. These phase transformations may be investigated in a number of ways including calorimetry, thermogravimetry, spectrometry and crystalline structure analysis. For example, it is clear from the crystal structure that the caffeine molecule possesses a hydrophilic centre at the iminazole nitrogen atom, N9, susceptible to H-bonding and that the hydrate water molecule effloresces *via* a molecular escape tunnel through the crystallographic *a*-face of the lattice (space group $P2_1/c$)[1,2] [see Fig. 1 (*a*)]. The crystalline hydrate is known to be non-stoichiometric in terms of its water content and under ambient atmospheric conditions transforms over several days to the anhydrous β-phase. The stability of the hydration is of considerable interest and may be compared to that of its nearest analogues theophylline, 1,3-dimethyl-7*H*-purine-2,6-dione,[2] [Fig. 1(*b*)] and 1,7,9-trimethylpurine-2,6-dione[3] [Fig. 1(*c*)]. The limited solubility of caffeine in water (Table 1) and ethanol contrasts with its free solubility in chloroform, and points to a distinctive hygroscopicity, a feature of the polarity of the molecule and its stereospecific attachment to water (Fig. 2), which is a significant physicochemical property of this food and drug reagent.[4,5] The polycrystalline anhydrous β-phase will metamorphose on heating and then by sublimation form crystals of the α-phase, which will revert to the β-phase at room temperature. Consequently, discrimination of the phases is required for a reliable characterisation of the substance and its phase stability.

Experimental

β-Phase material (Lot 79F0469) was obtained from Sigma Chemicals Ltd., Poole, England (purity = 99.6%). Crystals of caffeine hydrate were obtained by slow recrystallisation from water and stored in a sealed vessel at 75% relative humidity in the presence of a NaCl saturated solution at room temp. Microcrystals of the α-phase material were prepared by slow sublimation of the β-phase at 155 °C.

The single crystal diffraction data were collected with a Stoe STADI4 four circle diffractometer (Stoe, Darmstadt, Germany) and the X-ray powder data (XRPD) collected with Stoe STADIP and Siemens D5000 diffractometers (Siemens, Germany).† Two trigonal space groups ($R\bar{3}$ and $R3$) were identified from sublimed microcrystals of mean dimension 0.04 × 0.01 ×

† Atomic coordinates, thermal parameters and bond lengths and angles have been deposited at the Cambridge Crystallographic Data Centre (CCDC). See 'Instructions for Authors', *J. Chem. Soc., Perkin Trans. 2*, 1997, Issue 1. Any request to the CCDC for this material should quote the full literature citation and the reference number 188/85.

Table 1 Thermochemical and hydration properties of caffeine and theophylline

Measurement	Anhydrous caffeine	Caffeine hydrate	Anhydrous theophylline	Theophylline hydrate
Density/g cm^{-3}	1.386 (0.012)	1.403 (0.001)	1.460[a] (0.002)	1.450[a] (0.007)
Hydrate water content TGA mol H_2O/mol of purine		0.78 (0.02)		0.99 (0.02[a])
KFT		0.82 (0.01)		1.00 (0.01)[a]
DSC		0.76 (0.06)		
Peak dehydration temp./°C		59.8 (2.4)		70.2 (0.4)[a]
Dehydration enthalpy/kJ mol^{-1}		31.2 (2.3)		49.7 (0.1)[a]
Activation energy of dehydration/ kJ mol^{-1} *N*-purge		58.5 (1.2)		70–90[a]
10% relative humidity		81.9 (1.1)		
20% relative humidity		156 (7)		
Solubility/g dm^{-3}, 298 K	22.9 (0.6)[a]	22.8 (0.7)[a]	10.5 (0.2)[a]	5.6 (0.4)[a]
303 K	25.7 (0.5)[a]		13.7 (0.3)[a]	
310 K	34.1 (1.0)[a]	32.3 (1.2)[a]	19.9 (0.3)[a]	12.6 (0.5)[a]
323 K	66.8 (1.2)[a]		39.6 (0.9)[a]	

[a] C. O. Agbada, Ph.D. Thesis, University of Bradford, 1991.

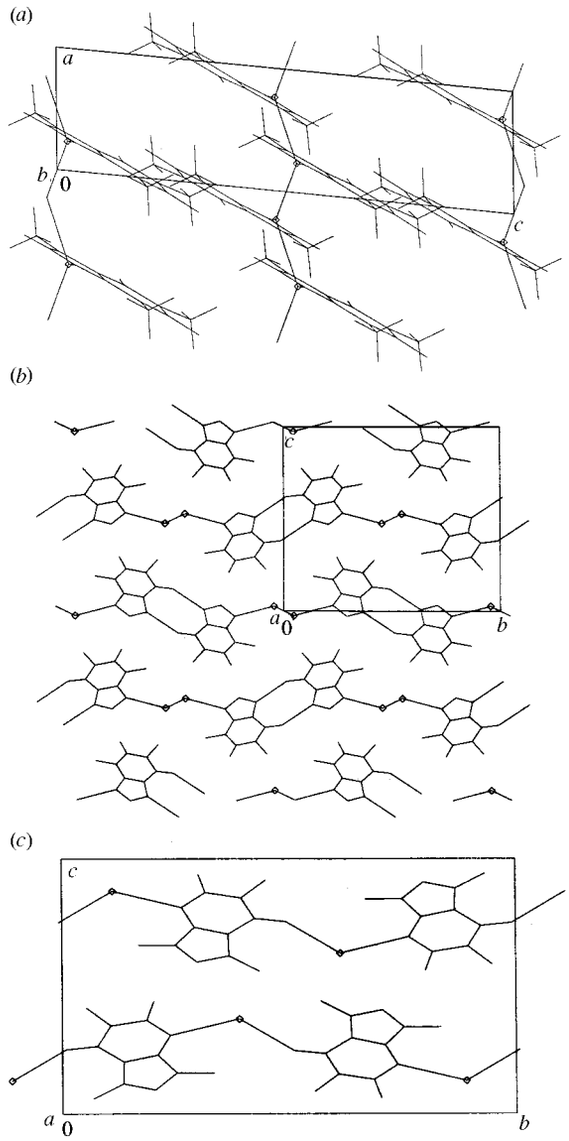

Fig. 1 (*a*) 1,3,7-Trimethylpurine-2,6-dione 'monohydrate' (caffeine hydrate). (*b*) Theophylline monohydrate, 1,3-dimethyl-7*H*-purine-2,6-dione monohydrate. (*c*) 1,7,9-Trimethylpurine-2,6-dione monohydrate.

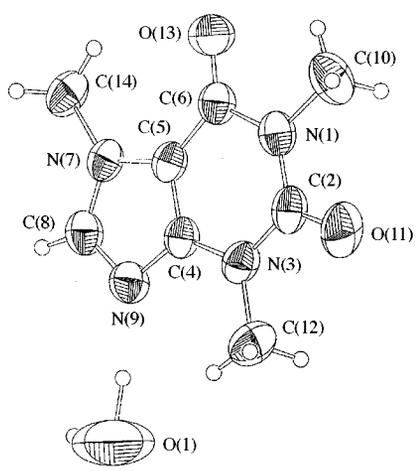

Fig. 2 Caffeine hydrate, 1,3,7-trimethylpurine-2,6-dione hydrate

0.01 mm of the α-anhydrous phase which proved to be very weak X-radiation scatterers. Structure determination on the limited number of reflections was accomplished with SHELXS-86 and SHELXL-93 programs.[6] A trial structure for the α-phase caffeine derived by rigid molecule refinement of the caffeine molecule in the *R*3 lattice was used for subsequent

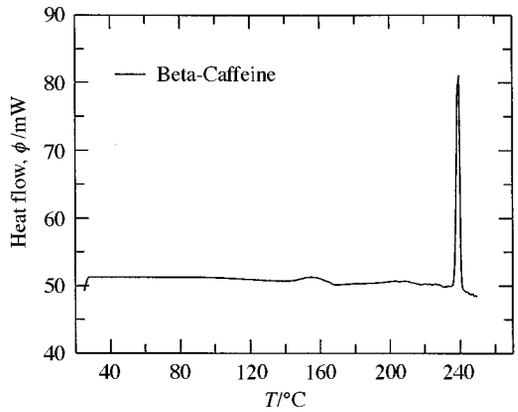

Fig. 3 DSC of the β- to α-anhydrous caffeine phase transition

Rietveld analysis of the anhydrous caffeine powders. Stoe STADIP Rietveld software was used for restricted parameter refinement of the lattice parameters and the hydrate content of the hydrate phase, and the lattice parameters for the β-anhydrous phase.

The phase transitions occurring between all the solid-state forms of caffeine were monitored using thermally resolved XRPD. Samples were heated using an Anton Paar thermal attachment (Anton Paar, Austria) and data collected at temperatures relating to the specific thermal events. The change in intensity of characteristic peaks relating to the hydrated and anhydrous phases were monitored during dehydration. The densities of α- and β-anhydrous phase and hydrated caffeine were determined using helium pycnometry.

The water content of caffeine hydrate was determined using the conventional methods of thermogravimetric analysis (TGA 7, Perkin-Elmer, Norwalk, USA) and Karl–Fischer titrimetry (KFT, Metrohm, Switzerland). In addition, enthalpies of dehydration acquired from differential scanning calorimetry (DSC 7, Perkin-Elmer) were used to calculate the molar content of water[7] eqn. (1) where η = molar water content, h_d = specific

$$\eta = h_d M_s/(h_v - h_d)M_w \quad (1)$$

heat of dehydration (J g^{-1}), M_s = relative molecular mass of anhydrous caffeine (~194 g mol^{-1}), h_v = specific heat of vaporisation of water = 2261 J g^{-1}, M_w = relative molecular mass of water.

Transitions in the molecular environment and arrangement of caffeine during water loss were detected using FT Raman spectroscopy. The sample was heated at 30, 35 and 40 °C using an environmental chamber. Measurements of 200 scans were obtained at 5 min intervals in the range 50–3500 cm^{-1} at a resolution of 4 cm^{-1}. The spectra were recorded on a Bruker FRA 106-FT Raman spectrometer (Bruker, Germany) using an Nd:YAG laser with a wavelength of 1064 nm.

Differential scanning calorimetry was used to investigate the dehydration and the β- to α-phase transition (Fig. 3). From the derived data a peak transition temperature (155.25 ± 1.2 °C) and enthalpy of transition (3.6 ± 1.2 kJ mol^{-1}) were calculated. The dehydration kinetics of caffeine hydrate were monitored using isothermal thermogravimetry. The samples were heated at isothermal temperatures both under dry nitrogen purge (TGA 7, Perkin-Elmer, Norwalk, USA) and at controlled relative humidity using a moisture balance (CI Electronics, Salisbury, UK). The derived data were fitted to mathematical equations of solid state decomposition.[8] Conformity of the data to three-dimensional diffusion (Jander) under dry nitrogen and a first-order mechanism at elevated humidity was confirmed using least-squares correlation coefficients ($r \geqslant 0.990$). These mechanisms correspond with those designated by Griesser and Burger for the dehydration of caffeine hydrate under conditions of various relative humidity.[9] Dehydration rate constants were

fitted to the Arrhenius relationship and activation energies of dehydration were subsequently calculated in order to assess hydrate stability (Table 1).

The crystal data for caffeine hydrate and the anhydrous α-phase caffeine is summarised in Tables 2 and 3. The molecular structure of caffeine hydrate is illustrated in Fig. 2.

Since β-phase single crystals were not available from crystallisation from water and organic solvents or sublimation, characterisation and identification of the β-phase crystal form was attempted by rigid molecule Rietveld refinement. Because of the similarity of the XRPD of the α-phase and β-phase caffeines, the space group ($P\bar{1}$) and starting lattice parameters were derived from the α-phase rhombohedral form determined by single microcrystal XRD analysis (Table 3) of the α-phase caffeine. The XRPD spectra are illustrated in Fig. 4 and derived crystalline parameters from the XRPD of the caffeine hydrate and anhydrous α- and β-phase caffeine are summarised in Table 4.

The XRPD spectra which are the usual means of phase identification of caffeine powders provide a convenient way for phase analysis and estimation of the variable hydrate content of these materials. Refinement of the crystalline water occupancy parameter of caffeine hydrate produced a value of 0.91(11) for comparison with the single crystal value of 0.84(1) moles of water per mole of caffeine.

Table 2 Crystal data and structure refinement for caffeine hydrate

Empirical formula	$C_8H_{12}N_4O_3$
Formula mass	212.22
T/K	293(2)
λ/Å	0.710 70
Crystal system	Monoclinic
Space group	$P2_1/c$
Unit cell dimensions	a = 3.9740(10), b = 16.751(4), c = 14.800(3) Å, β = 95.80(2)°
V/Å^3	980.2(4)
Z	4
D_c/Mg m^{-3}	1.438
Absorption coefficient/mm^{-1}	0.112
F(000)	448
Crystal size/mm	0.4 × 0.25 needle
θ range for data collection/°	1.84–24.96
Index ranges	$-4 \leqslant h \leqslant 4$, $-19 \leqslant k \leqslant 19$, $-17 \leqslant l \leqslant 17$
Reflections collected	3460
Independent reflections	1730 [R(int) = 0.0207]
Refinement method	Full-matrix least-squares on F^2
Data/restraints/parameters	1729/0/146
Goodness-of-fit on F^2	1.159
Final R indices [$I > 2\sigma(I)$]	$R1$ = 0.0591, $wR2$ = 0.1842
R indices (all data)	$R1$ = 0.0696, $wR2$ = 0.1967
Extinction coefficient	0.056(10)
Largest diff. peak and hole	0.386 and −0.327 e Å^{-3}

Results and discussion

The single crystal data for caffeine hydrate confirms, more accurately, the basic structure reported by Sutor in 1958.[2] The hydrate O1 to purine N9 hydrogen bond distance is 2.816(4) Å and the degree of occupancy of the hydrate site for a freshly prepared or stored as described sample is 0.84(1). The hydration enthalpy is low (31.2 kJ mol^{-1}) compared to that of its analogue theophylline monohydrate (49.7 kJ mol^{-1}). Corresponding differences in dehydration activation energies for measurements under dry nitrogen are also apparent (Table 1). The low value for the enthalpy of conversion (−3.6 kJ mol^{-1}) of the α-phase to the β-phase at 155 °C indicates that only a slight relaxation of the crystal packing is required for this transformation (see Fig. 3). The cohesive lattice bond of anhydrous caffeine lacks a conventional lattice hydrogen bond but Raman spectrometry (Table 5; Fig. 5) strongly indicates a CH to O hydrogen bond, which is apparent in the $R\bar{3}$ α-phase structure (Fig. 6).

Upon heating the caffeine hydrate sample, dehydration occurred, during which the non-stoichiometric molecular water content was released *via* the molecular escape tunnel which is suggested from the crystal structure determination. This phenomenon induces specific changes in derived spectra. General shifts in vibrational peak positions were ascribed to crystal collapse due to dehydration and subsequent molecular rearrangement.

Several minor spectral changes involve the imidazole ring resulting from the cleavage of the solitary existing hydrogen bond between the water of crystallisation and the caffeine mol-

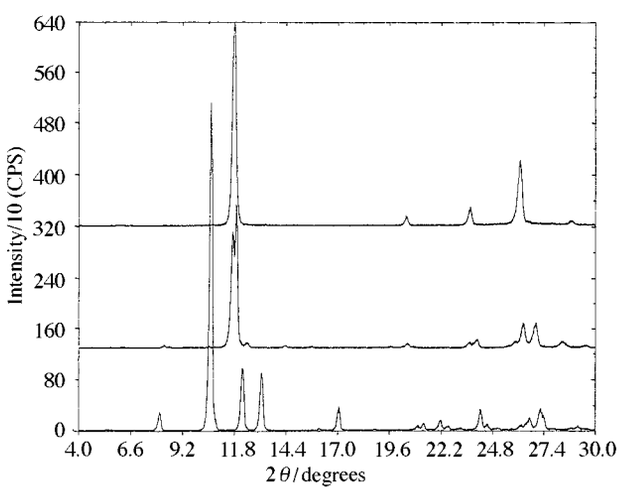

Fig. 4 XRPD of caffeine hydrate (lower trace), β-phase caffeine (middle trace), α-phase caffeine (upper trace)

Table 3 Crystal data and structure refinement for the α-phase anhydrous caffeine

Empirical formula	$C_8H_{10}N_4O_2$	$C_8H_{10}N_4O_2$
Formula mass	194.20	194.20
T/K	293(2)	293(2)
λ/Å	1.5418	1.5418
Crystal system	Trigonal	Trigonal
Space group	$R\bar{3}$	$R3$
Unit cell dimensions	a = 14.970(10), b = 14.970(10), c = 6.930(10) Å, α = 90, β = 90, γ = 120°	a = 14.970(10), b = 14.97(10), c = 3.470(10) Å, $\alpha = \beta$ = 90, γ = 120°
V/Å^3	1345(2)	673(2)
Z	6	3
D_c/Mg m^{-3}	1.439	1.437
Crystal size/mm	0.04 × 0.01 × 0.01	0.04 × 0.01 × 0.01
Refinement method	Rigid molecule refinement on F^2	Rigid molecule refinement on F^2
Data/restraints/parameters	406/0/31	195/16/57
Goodness-of-fit on F^2	5.249	2.628
Final R indices [$I > 2\sigma(I)$]	$R1$ = 0.2859, $wR2$ = 0.6754	$R1$ = 0.1353, $wR2$ = 0.3393
Largest diff. peak and hole	0.357 and −0.366 e Å^{-3}	0.213 and −0.187 e Å^{-3}

Table 4 X-Ray diffraction powder reliability factors, hydrate content and lattice parameter refinement of anhydrous an hydrate phase caffeine

	α-Phase	α-Phase[a]	β-Phase	Hydrate
Space group	$R3$	$R\bar{3}$	$P\bar{1}$	$P2_1/c$
Z	1	2	2	4
a/Å	8.7197	8.9463	9.4134(6)	3.9739(1)
b/Å	8.7197	8.9463	9.4089(9)	16.7560(4)
c/Å	8.7197	8.9463	8.8559(4)	14.7924(4)
α/°	118.276	113.578	108.738(5)	90
β/°	118.276	113.578	112.224(3)	95.820(2)
γ/°	118.276	113.578	120.697(7)	90
V/Å^3	224.00	448.32	476.51	979.91
D_c/Mg m^{-3}	1.439	1.439	1.354	1.424
D(exp.)/Mg cm^{-3}	1.387(1)	1.387(1)	1.386(12)	1.403(1)
H_2O occupancy				0.91(12)
R_p	0.2181	0.1747	0.2026	0.0862
R_{wp}	0.2755	0.2400	0.2883	0.1122

[a] The parameters of the $R\bar{3}$ hexagonal form from the single crystal data were transformed to R rhombohedral form for the purpose of this calculation and these parameters were relaxed for refinement of the $P\bar{1}$ lattice parameters of the β-phase. $R_p = \Sigma(I_{obs} - I_{calc})/\Sigma I_{obs}$ where I = Intensity at each reflection point; $R_{wp} = \sqrt{[\Sigma_w(I_{obs} - I_{calc})^2/\Sigma\omega I_{obs}^2]}$ where w = mean unit weighting at each reflection point, R_{wp} is regarded as the most significant parameter since this is the factor which is minimised in the refinement procedure.

Table 5 Raman spectra of hydrated and anhydrous crystalline caffeine

Hydrate		Anhydrous	
ν/cm^{-1} and vibrational assignment	Comments	ν/cm^{-1} and vibrational assignment	Comments
3121m ν =CH	Shifts to 3113 cm^{-1}	3113m ν =CH	
3026w	Resolution decreases		
3009w			
2955m ν CH_3	Intensity increases upon dehydration and shifts to 2957 cm^{-1}	2957s ν CH_3	
1698s ν C=O		1698s ν C=O	
		1656m ν C=O	Observed in hydrate but very weak. Large relative intensity increase with respect to 1697.7
1605s ν C=C	A slight decrease in intensity shifting to 1600 cm^{-1}	1600m ν C=C	
1551w ν C−C	Shift to 1554 cm^{-1}	1554w ν C−C	
1475w δ CH	Decreasing resolution becoming small shoulders within a broad peak	1456sh ν C=N	Increase in wavenumber due to loss of water interaction
1454w ν C=N			
1409m ν CN	Shifts to 1408 cm^{-1}	1408w ν CN	
1361m ν CN		1360m ν CN	
1333s ν CN	Shifts to 1328 cm^{-1}	1328s ν CN	
1290m ν CN	Shifts to 1284 cm^{-1}	1284m ν CN	
1255m δ H−C=N	Recedes to a shoulder upon dehydration		
1242m	Shifts to 1241 cm^{-1}	1241m	
1076w in plane δ C−C	Shifts to 1073 cm^{-1}	1073w in plane δ C−C	
930w δ imidazole ring	Shifts to 928 cm^{-1}	928w δ imidazole ring	
890w λ H_2O	Disappears upon dehydration		
805w	Shifts to 801 cm^{-1}	801w	
744m	Shifts to 741 cm^{-1}	741m	
647m δ O=C−N	Shifts to 644 cm^{-1}	644m δ O=C−N	
555s δ O=C−N		556s δ O=C−N	

s = strong, m = medium, w = weak, sh = shoulder, ν = stretch, δ = deformation, λ = libration.

ecule. N9 of the caffeine molecule accepts a hydrogen from the water to form this intermolecular interaction which upon cleavage causes a change in molecular environment of the imidazole ring, leading to significant changes in spectroscopic properties.

The spectrum representing the fully hydrated sample (Fig. 5) shows sharp well-defined peaks typical of a rigid structure. The caffeine molecules are supported by a spine of water molecules in a hydrogen bonded polymeric chain as concluded from crystallographic investigation. The instability of this chain arises from the weakness of its intermolecular bonds in contrast to the strong intermolecular H-bonds of its analogues theophylline monohydrate and 1,7,9-trimethylpurine-2,6-dione monohydrate (Fig. 1). Additionally, the vacancies within these zig-zag hydrate chains allows a more facile movement of the water molecules. Dehydration occurs quite rapidly at 40 °C, with the majority of alterations to spectra commencing simultaneously. This suggests that molecular rearrangement occurs promptly after hydrogen bond cleavage.

In order to confirm the assignments of individual vibrational bands, the spectra were compared to those of purine,[10,11] imidazole,[12] triazine[13–15] and pyridine.[16] Examination of the spectra in the CH stretching region shows a reduction in wavenumber of the =CH stretch at 3121 cm^{-1} with corresponding broadening. The final position of the band is indicative of the increase in intensity of a new =CH vibration at lower wavenumber which is produced as a result of intermolecular association of the C8H group. This is mirrored by a decrease in resolution of the peaks at 3026 and 3009 cm^{-1} which are not fundamental bands but are related to the original =CH stretch. The C=C stretch at 1605 cm^{-1} shifts to lower wavelength, emphasising a slight change in orientation of this bond as the water of crystallisation is lost. The relatively large intensity increase of the C=O

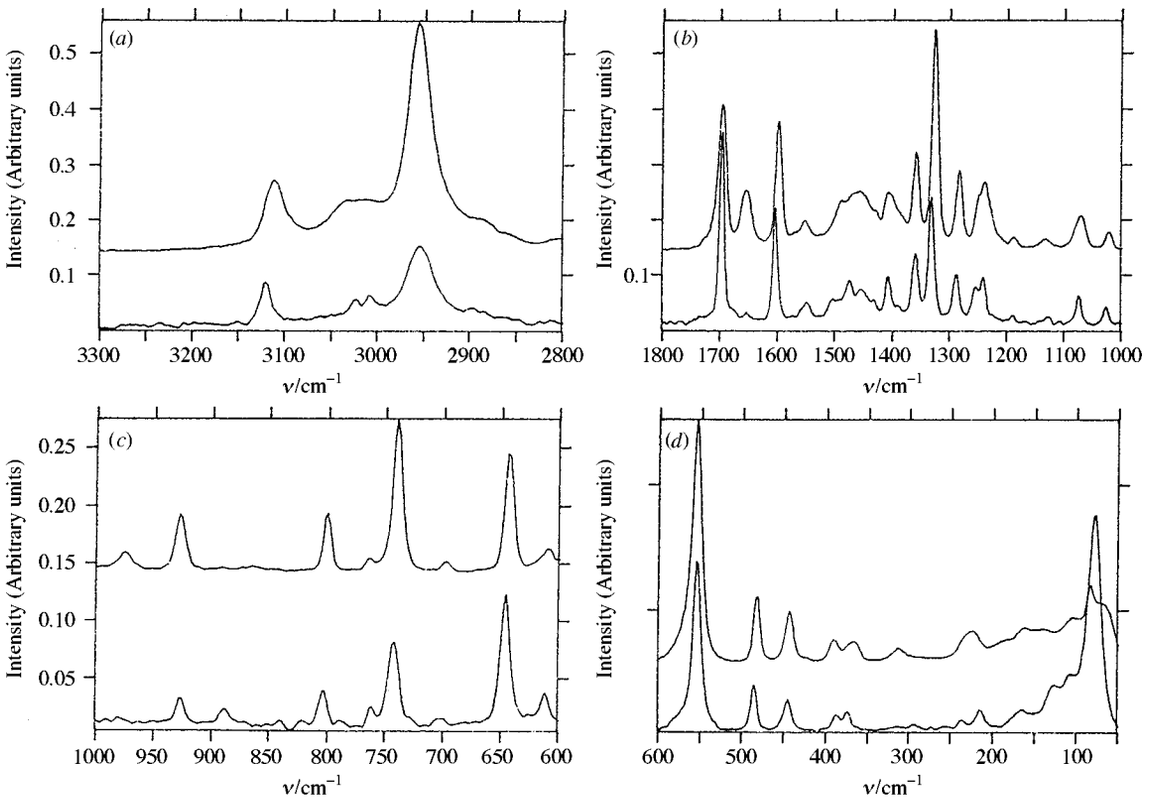

Fig. 5 Raman spectra of caffeine hydrate (lower trace) and β-phase anhydrous caffeine (upper trace). (*a*) Wavenumber region 3300–2800 cm^{-1}, (*b*) wavenumber region 1800–1000 cm^{-1}, (*c*) wavenumber region 1000–600 cm^{-1} and (*d*) wavenumber region 600–50 cm^{-1}.

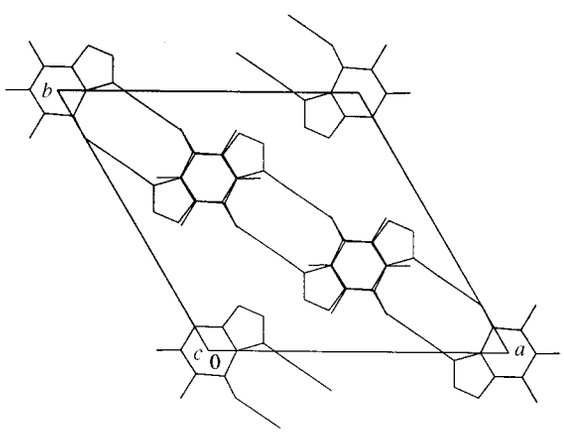

Fig. 6 CH···O Hydrogen bonding in the α-caffeine $R\bar{3}$ trigonal structure

stretch observed during dehydration at 1656 cm^{-1} is indicative of an alteration in the environment of one of the carbonyl groups situated on the pyrimidine ring. This result indicates the formation of a weak CH···O hydrogen bond which is apparent in the trigonal crystal structure of the α-phase caffeine.

Many authors have provided evidence for the formation of hydrogen bonds involving CH to O including the 1,7,9-trimethylpurine-2,6-dione monohydrate analogue with the C8 to O11 distance equal to 3.009(3) Å.[3] Rasmussen and Sletten concluded that there were no ordinary hydrogen bonds present in the structure of isocaffeine.[17] However, some of the C–H···O contacts between methyl and carbonyl groups may be classified as very weak hydrogen bonds. Shefter showed that there are two short intermolecular interactions that appear to be joining the molecules of 5-chlorosalicylic acid and caffeine in chains throughout the crystal lattice of the 1:1 complex.[18] These are between (5-chlorosalicylic acid)C4–H···O=C6 (caffeine) and C8H···O=C2 which hold individual caffeine molecules together. The C8H···O11 distance in caffeine hydrate of 3.18 Å is too large for the occurrence of hydrogen-bonding, in the anhydrate phases, however, in the absence of a conventional hydrogen bond a weak intermolecular hydrogen-bond arises between CH3···O 2.90(5) Å (Fig. 6).[19] Additionally, Krimm showed spectroscopically that C–H···O=C bonding plays a significant role in the stability of polypeptides,[20] whilst Dulmage and Lipscomb, and Dougill and Jeffrey provided evidence for weak associations involving C–H in hydrogen cyanide and dimethyl oxalate respectively.[21,22]

Of particular spectroscopic interest are changes involving nitrogen, since these reflect the loss of hydrogen donation by the water molecule and thus justify the alterations within the appropriate spectral regions. Applicable changes include the loss of resolution of the weak C=N stretch 1454 cm^{-1} which shifts to higher wavenumber, recession of the H–C=N deformation at 1255 cm^{-1}, and a shift to lower wavenumber of the weak imidazole ring vibration at 930 cm^{-1}. The lattice vibrations occurring in the region <200 cm^{-1} change dramatically as the hydrated lattice is destroyed. The concomitant disappearance of a water libration is also observed at 890 cm^{-1}, which supports the hypothesis of molecular realignment associated with corresponding loss of water of crystallisation.

References

1 S. R. Byrn, *Solid State Chemistry of Drugs*, Academic Press, London, 1982.
2 D. J. Sutor, *Acta Crystallogr.*, (*a*) 1958, **11**, 83; (*b*) 1958, **11**, 453.
3 M. Parvez and C. Ferguson, *Acta Crystallogr., Sect. C*, 1994, **50**, 1303.
4 R. Gerdil and R. E. Marsh, *Acta Crystallogr.*, 1960, **13**, 166.
5 P. R. Perrier and S. R. Byrn, *J. Org. Chem.*, 1982, **47**, 4671.
6 G. M. Sheldrick, 1993, University of Göttingen, 3400 Göttingen, Germany.
7 R. K. Khankari, D. Law and D. J. W. Grant, *Int. J. Pharm.*, 1992, **82**, 117.
8 J. H. Sharp, G. W. Brindley and B. N. N. Achar, *J. Am. Chem. Soc.*, 1966, **49**, 379.
9 U. J. Griesser and A. Burger, *Int. J. Pharm.*, 1995, **120**, 83.

10 M. Majoube, M. Henry and G. Vergoten, *J. Raman Spectrosc.*, 1994, **25**, 233.
11 M. Majoube, Ph. Millie, L. Chinsky, P. Y. Turpin and G. Vergoten, *J. Mol. Struct.*, 1995, **355**, 147.
12 J. Sadlej, *J. Mol. Struct.*, 1992, **274**, 247.
13 J. E. Lancaster and N. B. Colthup, *J. Chem. Phys.*, 1954, **22**, 1149.
14 S. J. Daunt, H. F. Shurvell and L. Pazdernik, *J. Raman Spectrosc.*, 1975, **4**, 205.
15 A. Navarro, J. J. Lopez Gonzalez, M. Fernandez Gomez, F. Marquez and J. C. Otero, *J. Mol. Struct.*, 1996, **376**, 353.
16 A. M. Heyns and M. W. Venter, *J. Chem. Phys.*, 1990, **93**, (**11**), 7581.
17 H. Rasmussen and E. Sletten, *Acta Chem. Scand.*, 1973, **27**, 2757.
18 E. Shefter, *J. Pharm. Sci.*, 1968, **57**(7), 1163.
19 D. J. Sutor, *J. Chem. Soc.*, 1963, 1105.
20 S. Krimm, *Science*, 1967, **158**, 530.
21 W. J. Dulmage and W. N. Lipscomb, *Acta Crystallogr.*, 1951, **4**, 330.
22 M. W. Dougill and G. A. Jeffrey, *Acta Crystallogr.*, 1953, **6**, 831.

Paper 7/02041D
Received 25*th March* 1997
Accepted 27*th May* 1997